Analysis of the Kinetics of Ovine Follitropin Agonist–Antagonist Interactions with Pig Ovarian Membranes†

K. Sebok,‡ A. De Léan,§ and M. R. Sairam*,‡

Reproduction Research Laboratory and Laboratory of Molecular Pharmacology, Clinical Research Institute of Montreal, 110 Pine Avenue West, Montreal, Quebec, Canada H2W 1R7

Received September 29, 1986; Revised Manuscript Received January 6, 1987

ABSTRACT: The binding of ^{125}I-labeled ovine follitropin (oFSH) and ^{125}I-labeled deglycosylated ovine follitropin (DG-oFSH) to porcine granulosa cell membranes was studied at equilibrium and nonequilibrium binding conditions and statistically analyzed. Saturation and competition binding experiments revealed homogeneity in the population of binding sites labeled with ^{125}I-oFSH, having a pK estimation of $\approx$10. ^{125}I-DG-oFSH similarly interacts with a single uniform class of receptors of equal affinity (p$K \approx 10$) and binding capacity as oFSH. In contrast, displacement experiments using ^{125}I-DG-oFSH as tracer and unlabeled oFSH as competing ligand demonstrate slope factors less than unity, suggesting apparent heterogeneity of sites not observed with ^{125}I-DG-oFSH vs. DG-oFSH competition experiments. Under these conditions, it appears that FSH binds to two sites in near equal proportion but of unequal affinities. The total specific binding capacities of these sites equal those observed in ^{125}I-DG-oFSH/unlabeled DG-oFSH competition experiments. Analysis of oFSH association kinetics at 37 °C by curve-fitting methods is best explained by a biexponential rate equation describing a fast and a slow association component that are equally distributed. DG-oFSH demonstrates a disproportionately greater amount of fast vs. slow binding component. The binding half-times for each component of oFSH and DG-oFSH are similar, i.e., minutes for the fast and hours for the slow $t_{1/2}$ times. At 37, 25, and 4 °C, DG-oFSH exhibits greater velocity of binding to the receptor than oFSH. Dissociation, promoted by the same unlabeled hormone, of bound ^{125}I-DG-oFSH and ^{125}I-oFSH induces biphasic kinetics consisting of a fast and a slow dissociable pool of prebound tracer. Computer analysis reveals that both tracers dissociate with similar fast $t_{1/2}$ times; however, DG-oFSH exhibited a $t_{1/2}$ approximately 2 times slower for the slower component vs. oFSH. From this study, it is concluded that oFSH and DG-oFSH bind to the receptor(s) in a complex reaction scheme, more so for oFSH than DG-oFSH. These differences in binding behavior may be the reason FSH is an effective agonist as opposed to DG-oFSH in activating the effector adenylate cyclase.

Although much work has been done to understand the nature of binding of follitropin (FSH)[1] with its receptor, this research has been centered primarily on the testicular FSH receptor. Means and Vaitukaitis (1972) first demonstrated specific uptake of FSH in immature rat testis using ^{3}H-hFSH. Other investigators further studied in detail the receptor binding properties of ^{125}I-hFSH to male rat testis (Abou-Issa & Reichert, 1976; Bhalla & Reichert, 1974; Fletcher & Reichert, 1984; Reichert & Bhalla, 1974; Reichert & Ramsey, 1975; Salhanick, 1980; Thanki & Steinberger, 1978) and bovine testis (Abou-Issa & Reichert, 1977; Anderson & Reichert, 1982; Cheng, 1975; Dias et al., 1984; O'Neill & Reichert, 1984). Some studies characterizing FSH binding to mouse (Davies et al., 1978), monkey (Berman & Sairam, 1982, 1984), porcine (Maghuin-Rogister et al., 1978), equine (Stewart & Allen, 1979), and human testicular tissue (Berman & Sairam, 1983) have also been documented. Adequate studies on the characterization of FSH–receptor interaction(s) in ovarian tissue of various sources are lacking. Initially, studies demonstrated specific uptake of iodinated FSH to rat granulosa cells using autoradiographic techniques (Midgley, 1973) or binding of ^{125}I-hFSH to receptors (Louvet & Vaitukaitis, 1976; Nimrod et al., 1976). Equilibrium and nonequilibrium FSH binding studies using the porcine granulosa cell model are lacking, although binding of ^{125}I-labeled hFSH to small, medium, and large porcine granulosa cells has been demonstrated (Labarbera & Ryan, 1981; Nakano et al., 1977). The availability of new analogues of FSH (Manjunath et al., 1982; Sairam & Manjunath, 1982a,b) that demonstrate lack of receptor-mediated induction of adenylate cyclase (Berman et al., 1985) and accumulation of cyclic AMP (Sairam & Manjunath, 1982a; Sairam et al., 1983), but enhanced apparent receptor affinity in gonadal tissue, spurred us to measure and compare the kinetic and equilibrium binding parameters of oFSH and deglycosylated oFSH (Manjunath & Sairam, 1984) in vitro, using porcine granulosa cell membranes. We have directed our attention to the method of analysis of the data and to the complexity of the binding reactions, with the hope that the differences uncovered may help further understand the dichotomies observed in postreceptor responses. This work is an extension of our previous reported results (Sebok et al., 1985).

Materials and Methods

Hormones and Chemicals. Highly purified ovine follitropin (oFSH) was isolated in this laboratory as described earlier (Sairam, 1979a). Deglycosylation of oFSH by anhydrous hydrogen fluoride was prepared by the procedure previously described (Manjunath & Sairam, 1982, 1984). Lactoper-

† These investigations were supported by the Medical Research Council of Canada (M.R.S. and A.D.L.).

* Correspondence should be addressed to this author.

‡ Reproduction Research Laboratory.

§ Laboratory of Molecular Pharmacology.

[1] Abbreviations: FSH, follitropin (follicle stimulating hormone); oFSH, ovine follitropin; DG-oFSH, deglycosylated ovine follitropin; hFSH, human follitropin; BSA, bovine serum albumin; PFF, porcine follicular fluid; Tris-HCl, tris(hydroxymethyl)aminomethane hydrochloride; EDTA, ethylenediaminetetraacetic acid; LH, luteinizing hormone; pK, $-\log K_D$.

0006-2960/87/0426-3650$01.50/0

oxidase and bovine serum albumin (BSA) were obtained from Sigma (St. Louis, MO). All other chemicals were of reagent grade from Fisher Scientific Co. (Montreal, Canada).

Iodination of Hormones. The oFSH and DG-oFSH preparations were labeled with ^{125}I by the lactoperoxidase method, as described elsewhere (Sairam, 1979b). The labeled oFSH and DG-oFSH had specific activities of 74–91 and 60–116 $\mu Ci/\mu g$, respectively, and were generally used within 2 weeks of preparation.

Preparation of Porcine Granulosa Cell Membranes for Radioligand–Receptor Assay. Porcine follicular fluid (PFF) supplied by the Contraceptive Development Branch, NICHHD (Bethesda, MD), was stored at −70 °C until used. In preparation of the receptor for binding studies, the contents (PFF) in the bottles were allowed to thaw under a stream of cold air. All additional procedures were performed at 4 °C. The PFF was first centrifuged at 13342*g* in a Beckman J-21B centrifuge for 30 min. The supernatant fraction containing the clear fluid was removed, and the pellet consisting of cellular debris (mostly of free floating granulosa cells at the time of collection) was resuspended in 25 mM Tris-HCl buffer, pH 7.2, containing 1 mM ethylenediaminetetraacetic acid (EDTA) and 100 mM sucrose. Cells were disrupted by using a hand-held ground-glass homogenizer. The homogenate was recentrifuged at 30000*g* for 30 min at 4 °C. The supernatant was discarded, and resultant pellet was disrupted, washed in 25 mM Tris-HCl buffer, pH 7.2, containing 10 mM $MgCl_2$, and recentrifuged for 30 min at 30000*g*. The pellet P1 representing the membranes was then resuspended by using a ground-glass homogenizer in 25 mM Tris-HCl (pH 7.2) containing 10 mM $MgCl_2$. Aliquots of the P1 fraction were stored at −70 °C. Before use, the P1 membrane fraction was thawed, diluted, and gently resuspended in the assay buffer by use of a glass homogenizer.

Protein Estimation. To determine protein content, 100-μL samples of the P1 fraction, either diluted or undiluted, were mixed with 100 μL of 0.5 M NaOH and heated in a boiling water bath for 30 min. Following the incubation, 100 μL of 0.5 M HCl was added, and the amount of protein was determined by using a Bio-Rad protein assay kit (Bio-Rad, Richmond, CA). Bovine serum albumin was used as the standard.

^{125}I-Labeled oFSH and DG-oFSH Saturation Binding Assays.[2] Assays were conducted with 75 × 11 mm disposable polystyrene tubes. Tubes were kept chilled on ice, and the following reagents were added: first, 100 μL of assay buffer (pH 7.2) consisting of 25 mM Tris-HCl containing 10 mM $MgCl_2$ and 0.1% bovine serum albumin ± 500 ng of unlabeled homologous hormone; next, 100 μL of assay buffer containing various concentrations of either ^{125}I-oFSH or ^{125}I-DG-oFSH; and last, 100 μL of assay buffer containing the P1 membrane fraction. The final reaction volume was 300 μL. Following agitation with a vortex mixer, all tubes were incubated in a continuously shaking Dubnoff water bath at 37 °C. The binding reaction was allowed to occur until equilibrium binding was obtained. This occurred sooner for DG-oFSH than oFSH (see Results). Following incubation, the reactions were quenched by the addition of 2 mL of assay buffer (4 °C) and clarified by centrifugation at 2900*g* for 10 min at 4 °C in a table-top IEC clinical centrifuge. The supernatant was aspirated under vacuum and discarded, and the radioactivity in the pellet was determined by using an LKB Rackgamma II counter with 70% counting efficiency for ^{125}I.

Radiolabeled oFSH and DG-oFSH Competition Binding Assays. The binding of ^{125}I-oFSH or ^{125}I-DG-oFSH to membranes occurred at equilibrium or nonequilibrium conditions, as specified in text. At 37 °C, the reaction was initiated by the addition of the P1 membrane fraction to test tubes containing assay buffer, as described, a low fixed concentration of ^{125}I-ligand, and titrated amounts of homologous unlabeled competitor. Concentrations of oFSH or DG-oFSH ranged from 1.24×10^4 pM (100 ng) to 6.06 pM (≈48 pg) or 1.38×10^4 pM (100 ng) to 6.77 pM (≈48 pg), respectively. Nonspecific binding was determined in the presence of 500 ng of unlabeled DG-oFSH or oFSH. At the end of the incubation period, as specified in figures, bound ligand was separated from free by centrifugation following quenching of the reaction by addition of 2 mL of chilled (4 °C) assay buffer.

Isotherms as a Function of Ligand Concentration. To a series of 11 × 75 mm test tubes containing assay buffer, as described, and aliquots of P1 membrane fraction, various concentrations of either ^{125}I-labeled DG-oFSH or oFSH (as indicated in Figure 2) were quickly added, and the incubates (300 μL) were placed in a water bath at 37 °C. At selected intervals between 0 and 600 or between 0 and 420 min, for oFSH and DG-oFSH, respectively, the reaction was quenched with 2 mL of ice-cold assay buffer. Bound and free tracer were separated and counted as described above.

Time and Temperature Dependence of Binding of ^{125}I-DG-oFSH and ^{125}I-oFSH to the P1 Membrane Fraction at 37, 25, and 4 °C. Duplicate or triplicate determinations were performed to test the level of specifically bound ^{125}I-labeled oFSH or DG-oFSH. The assay mixture (300 μL) consisted of 35 μL (≈30 μg of protein equivalent) of P1 fraction, 25 mM Tris-HCl buffer (pH 7.5), 10 mM $MgCl_2$, 0.1% BSA, and 70959 cpm (≈0.48 ng; 66.0 pM) of ^{125}I-DG-oFSH or 74865 cpm (≈0.52 ng; 65.0 pM) of ^{125}I-oFSH. In all cases, nonspecific binding was determined in the presence of 11.6 nM unlabeled oFSH. The tubes were incubated at a water bath at three temperatures (4, 25, and 37 °C) for selected time intervals up to 12 or 24 h. Reactions were terminated, and bound vs. free tracer was separated by the method previously mentioned.

Dissociation Kinetics of ^{125}I-Labeled oFSH and DG-oFSH. In order to determine the time course of dissociation of both ^{125}I-labeled tracers, two experimental protocols were used. The first protocol had three separate reaction vessels, incubated in a water bath at 37 °C, with sufficient amounts of labeled hormone, assay buffer, and P1 fraction added so that a 300-μL aliquot could be removed sequentially, as indicated in the figures, during the incubation period. For each radiolabeled ligand, the experiment was first initiated by using two reaction vessels, designated group I and group II. Group I defined the amount of total binding of either ^{125}I-labeled oFSH or DG-oFSH. This binding included specific binding to receptor sites and nonspecific binding to sites on the pellet and test tube in the absence of the same but unlabeled hormone. Group II incubate was used to determine the level of nonspecific binding in the presence of 100 ng per 300-μL aliquot of unlabeled oFSH or DG-oFSH. Following an 80-min preincubation period, a predetermined volume of group I reaction mixture was removed, placed in a third empty incubation vessel, and designated group III. Dissociation of prebound radiolabeled ligands from FSH receptor contained in the group III reaction vessel was promoted immediately after the 80-min preincubation period, transfer, and addition of a 1000 ng per 300-μL aliquot of the same but unlabeled hormone. The incubation

[2] Specificity of binding was established when purified oLH or hCG, or their deglycosylated counterparts, did not compete significantly, except at extremely high concentrations.

was continued up to 500 min, during which time 300-μL samples were removed to determine the amount of ^{125}I-labeled tracer still bound to FSH receptor.

To determine the dissociability of bound ^{125}I-labeled oFSH and DG-oFSH to receptor sites following incubation at two selected preequilibration time intervals, the assay conditions were as described for the association kinetic experiment. At 30- or 120-min incubation time, 1000 ng of the same but unlabeled hormone was added.

Analysis of Equilibrium and Nonequilibrium Binding Data. Experimental binding data from saturation experiments at equilibrium were analyzed by using the computerized program LIGAND described by Munson and Rodbard (1980). Competition curves were analyzed first by the four-parameter logistic equation as described by De Lêan et al. (1978) to determine the steepness factor of the curves. The experimental data were then subjected to nonlinear least-squares curve fitting using a generalized model for complex ligand–receptor systems as described by Feldman (1972). In the determination of the binding capacity (R) and the association equilibrium constant (K_A), the molecular weight of oFSH was considered to be 28 600 and 24 000 for deglycosylated ovine follitropin preparations (Manjunath et al., 1982). Where necessary, data were analyzed for significance by the Student's t test.

The time course of association of radioligand to receptor sites was analyzed by one or several exponential terms based on the equation $B_t = a_0 + \sum a_i[1 - \exp(-b_i t)]$ where a_0 is nonspecific binding, a_i is the size of exponential component i with time constant b_i, and t is incubation time. The time course of dissociation was similarly analyzed according to the equation $B_t = \sum a_i \exp(-b_i t)$ where all parameters have the same meaning as for association time courses. The time constant of dissociation (K_{off}) was directly obtained from the estimate for b_i, while the rate of association, a term equal to the sum of the second-order rate constant of association of labeled ligand (L) multiplied by the ligand concentration plus the first-order dissociation rate constant, is similarly obtained from the b_i estimate given in the first equation.

In this study, the definition of percent specific binding is $(B_0 - NS)/B_t \times 100$, given B_0 = total counts bound to pellet and test tube, B_t = total radioactivity added per assay tube, and NS = total counts bound in the presence of a large excess of unlabeled hormone.

RESULTS

Analysis of the Kinetic Binding Data. The rate of association for each radiolabeled ligand to the FSH receptor is markedly influenced both by the duration and by the temperature of the incubation medium. Both ligands showed higher rates of association to the binding site(s) at 37 °C, than at 24 and 4 °C. Specific binding of both radiolabeled ligands did not noticeably decline with prolonged incubation (i.e., 12–24 h) even at 37 °C (Figure 1). At 24 and 4 °C, ^{125}I-DG-oFSH and ^{125}I-oFSH failed to reach binding equilibrium; however, during earlier phases of association, the deglycosylated FSH preparation consistently exhibited greater amounts of specific binding than oFSH at each time point. At 37 °C and equal molar concentrations, ^{125}I-DG-oFSH asymptotically approached steady state of binding sooner (≈ 2–4-h incubation) than ^{125}I-oFSH (≈8 h). Equilibrium binding occurred at various times depending on the batch of P1 fraction and the amount of tracer added, but in all situations, DG-oFSH reached equilibrium binding sooner. Binding isotherms at 4 and 25 °C are not shown.

The kinetics of ^{125}I-labeled DG-oFSH and oFSH binding to the P1 fraction when plotted to pseudo-first-order kinetics indicate the association reaction could not be fitted to a simple bimolecular reaction, since both curves deviated from linearity (plots not shown).

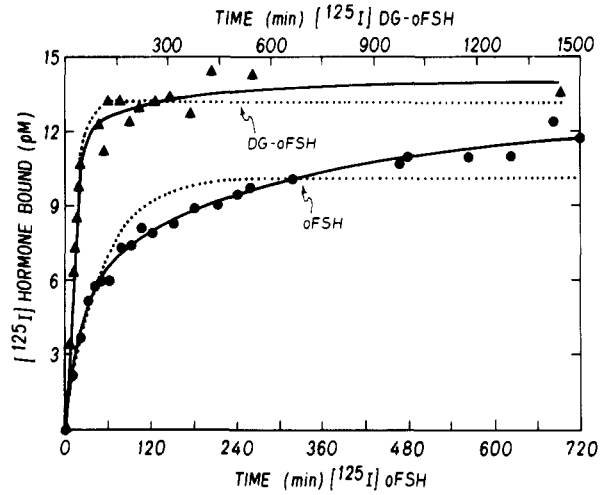

FIGURE 1: Time course of association of 65.0 pM ^{125}I-oFSH and 66.0 pM ^{125}I-DG-oFSH, at 37 °C, to porcine ovarian FSH receptor. The assay tubes contained ^{125}I-labeled hormones, ≈30 μg of protein equivalent of P1 fraction, and assay buffer ± 100-fold excess unlabeled oFSH (11.6 mM) at a final volume of 300 μL. Data points are the mean total binding of triplicate determinations. Dotted and solid curves represent the time course of association fitted to a mono- or biexponential equation, respectively.

Table I: Results of Analysis of the Time Course of ^{125}I-Labeled oFSH and DG-oFSH Binding to Porcine Granulosa Cell Membranes at 37 °C[a]

Experiment 1: 66.0 pM ^{125}I-DG-oFSH/Tube		
b_1 = 0.044 ± 0.04 min^{-1}	(fast) $t_{1/2}$ = 16 min	a_1 = 88%
b_2 = 0.003 ± 0.004 min^{-1}	(slow) $t_{1/2}$ = 231 min	a_2 = 12%
Experiment 2: 69.0 pM ^{125}I-DG-oFSH/Tube		
b_1 = 0.30 ± 0.10 min^{-1}	(fast) $t_{1/2}$ = 2.3 min	a_1 = 73%
b_2 = 0.014 ± 0.003 min^{-1}	(slow) $t_{1/2}$ = 49 min	a_2 = 27%
Experiment 1: 65.0 pM ^{125}I-oFSH/Tube		
b_1 = 0.04 ± 0.004 min^{-1}	(fast) $t_{1/2}$ = 17 min	a_1 = 48%
b_2 = 0.0033 ± 0.00096 min^{-1}	(slow) $t_{1/2}$ = 210 min	a_2 = 52%
Experiment 2: 59.0 pM ^{125}I-oFSH/Tube		
b_1 = 0.065 ± 0.010 min^{-1}	(slow) $t_{1/2}$ = 11 min	a_1 = 52%
b_2 = 0.004 ± 0.003 min^{-1}	(slow) $t_{1/2}$ = 173 min	a_2 = 48%

[a] Values are the mean ± SEM. The table shows the values of a_1 (size of the fast exponential component expressed as a percentage of total specifically bound ligand), a_2 (size of the slow exponential component expressed as a percentage of total specifically bound ligand), and b_1 and b_2 [time constant (min^{-1}) of the fast and slow binding components]. $t_{1/2}$ represents the time (in minutes) required to bind 50% of the total ligand in either the fast or the slow association compartment. The diminution in the residual sum of squares going from a one-exponential binding model to a two-exponential binding model is highly significant in all cases, except in experiment 1: 66.0 pM ^{125}I-DG-oFSH/tube; in this instance, the data could be fitted by either a mono- or a biexponential equation.

Binding data for the association reactions for both tracers to receptor site(s), at 37 °C, where equilibrium was reached, were analyzed by using equations based on one or several exponential terms. ^{125}I-oFSH displayed a biphasic rate of association (Figure 1), showing about equal proportions of fast and slow rate components (Table I). The faster rate component of association was estimated to be 0.052 min^{-1} with a $t_{1/2}$ of binding estimated at ≈14 min (Table I). The $t_{1/2}$ for the slower component was estimated at ≈192 min, and its rate constant of association was ≈0.0037 min^{-1} (Table I).

Similar biexponential association kinetics were observed for ^{125}I-DG-oFSH. However, there is a significant difference in

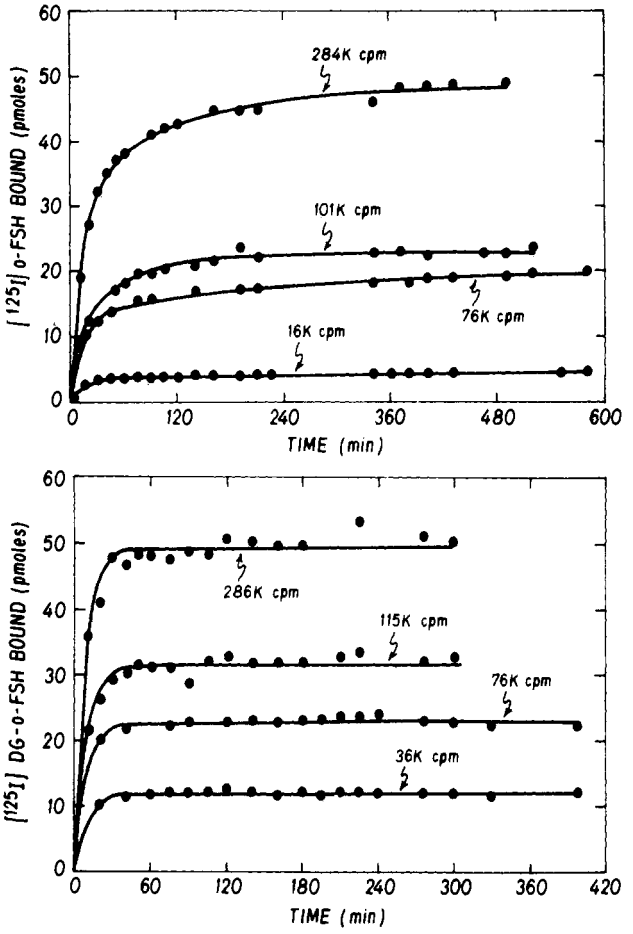

FIGURE 2: Effect of varying the initial concentrations of ^{125}I-oFSH and ^{125}I-DG-oFSH on the binding velocity to the P1 fraction at 37 °C. Varying concentrations of ^{125}I-labeled oFSH (81 μCi/μg) (e.g., 256 pM, 284 000 cpm, 2.2 ng; top panel) and DG-oFSH (84 μCi/μg) (e.g., 297 pM, 286 000 cpm, 2.1 ng; bottom panel) were added separately to ≈19 mg of protein equivalent of porcine ovarian P1 fraction and assay medium as described under Material and Methods ± 100 ng of unlabeled homologous hormone. Nonspecific (N.S.) binding (not shown) increased linearly and in proportion with increased ligand concentration. N.S. values for both tracers did not exceed 5–6% of the total labeled hormone added. Each point is the arithmetic mean of triplicate determinations that varied less than 2% or 5% from the mean for DG-oFSH and oFSH, respectively. The solid curves represent the binding isotherm calculated by using curve-fitting methods that best fit the experimental data points.

the proportion of fast vs. slow rate of association. The fast rate binding component comprises approximately 73–88% of the total specifically bound ligand, whereas the balance (12–27%) comprises the slower binding component (Table I). A representative association curve for ^{125}I-DG-oFSH is indicated in Figure 1. The estimates for the $t_{1/2}$ times for the fast and slow binding component are also in minutes and hours, respectively. The fast $t_{1/2}$ ranges from ≈3 to 16 min, whereas the slow $t_{1/2}$ ranges from 49 to 231 min.

Analysis of association binding kinetics at 37 °C of ^{125}I-labeled of oFSH to P1 fraction at various ligand concentrations revealed no change in either the fast or the slow rate constant of binding for oFSH. In the case of DG-oFSH, all association binding curves are best described by a monoexponential equation, having a fast rate constant of association that was independent of ligand concentration (Figure 2).

Analysis of the Binding, at Equilibrium, of ^{125}I-oFSH and ^{125}I-DG-oFSH to Porcine Granulosa Cell FSH Receptor at 37 °C. Figure 3 shows Scatchard plots of the concentration-dependent specific binding of ^{125}I-labeled oFSH and DG-oFSH under equilibrium conditions. The binding of ^{125}I-oFSH to homogenates of porcine granulosa cells was specific, saturable, and of high affinity. Computer-assisted analysis of the experimental binding data indicated that binding is described by a one-site model. In four experiments, using two different membrane preparations, the mean binding capacity is estimated at 27.7 ± 4.37 pM. Similar analysis of ^{125}I-DG-oFSH saturation curves indicates a model for a single class of high-affinity sites and a binding capacity of 36.8 ± 0.17 pM, n = 3. It may be noted that the binding capacities of both tracers are not significantly different ($p > 0.60$).

Competition for the ^{125}I-DG-oFSH Binding Site by Unlabeled DG-oFSH or oFSH. DG-oFSH competition curves at steady state were steep with a slope factor of near unity (Figure 4). Computer-assisted analysis of the DG-oFSH binding data using nonlinear curve-fitting methods indicated that the curves were most consistent with a one-site model vs. a two-site model. The K_A of DG-oFSH determined in this manner was (0.862 ± 0.187) × 10^{10} M^{-1} (n = 5).

Binding of ^{125}I DG-oFSH to FSH receptor was inhibited by unlabeled oFSH in a concentration-dependent manner. The displacement curve for oFSH, indicated in Figure 4, was performed by using a "fast" binding tracer (DG-oFSH) and a "slow" equilibrating competitor (oFSH). Time course analysis of the binding of ^{125}I-oFSH at 37 °C indicated specific binding at 2.5 h had not reached equilibrium; however, at this time, at equal molar concentration, equilibrium binding for ^{125}I-DG-oFSH had occurred. Under these nonequilibrium conditions for oFSH, the displacement curves were shallow with a slope factor less than unity (i.e., 0.6–0.7, n = 2). When the experiment was repeated (Figure 5), with the incubation interval extended long enough for equilibrium binding to be established for ^{125}I-labeled oFSH (i.e., ≈7 h), no marked change was observed in the steepness of the slope, i.e., 0.647 (2-h period; n = 2) vs. 0.747 (7-h period; n = 2). Under identical assay conditions and incubation periods, the ^{125}I-DG-oFSH/DG-oFSH competition curve had a slope factor that was unchanged, i.e., 1.04 (2 h; n = 2) vs. 1.07 (7 h; n = 2) (Figure 5).

On the basis of the lack of change in the slope factor at the two time periods, the results from the analysis of oFSH displacement curves of the above experiments were combined. Assuming a state of equilibrium binding, a two-site model most consistently fitted the data vs. a one-site model. The experimental data reveal a population of sites in which 40–60% of the binding is of high affinity and 45–55% of the remainder was of a form exhibiting low equilibrium binding affinity. It was observed that the total binding capacities of the high (R_H) but poorly defined [$K_A \approx (0.63 \pm 0.24) \times 10^{10}$ M^{-1}, n = 4; $R_H \approx 45 \pm 4.1$ pM, n = 4] and low [$K_A \approx (2.0 \pm 0.55) \times 10^8$ M^{-1}, n = 4; $R_L \approx 47 \pm 7.7$ pM, n = 4] affinity sites equaled the binding capacity ($R_H \approx 90 \pm 9.2$ pM, n = 4) of the "indiscriminate" form of the receptor to DG-oFSH, as determined from ^{125}I-DG-oFSH vs. unlabeled DG-oFSH competition assays.

Competition for the ^{125}I-oFSH Binding Site by Unlabeled DG-oFSH and oFSH. At non-steady-state binding conditions for a slowly equilibrating system, inhibition of ^{125}I-labeled oFSH binding to porcine granulosa cell FSH receptors by unlabeled oFSH occurred in a concentration-dependent manner. Results of a typical competition assay are shown in Figure 6. The oFSH competition curves tend to be shallow and complex with slope factor less than 1 (i.e., 0.812; n = 2), suggesting an apparent heterogeneity in receptor population. Experiments were repeated using different P1 membrane fraction and tracer preparations and retested at a 7-h incu-

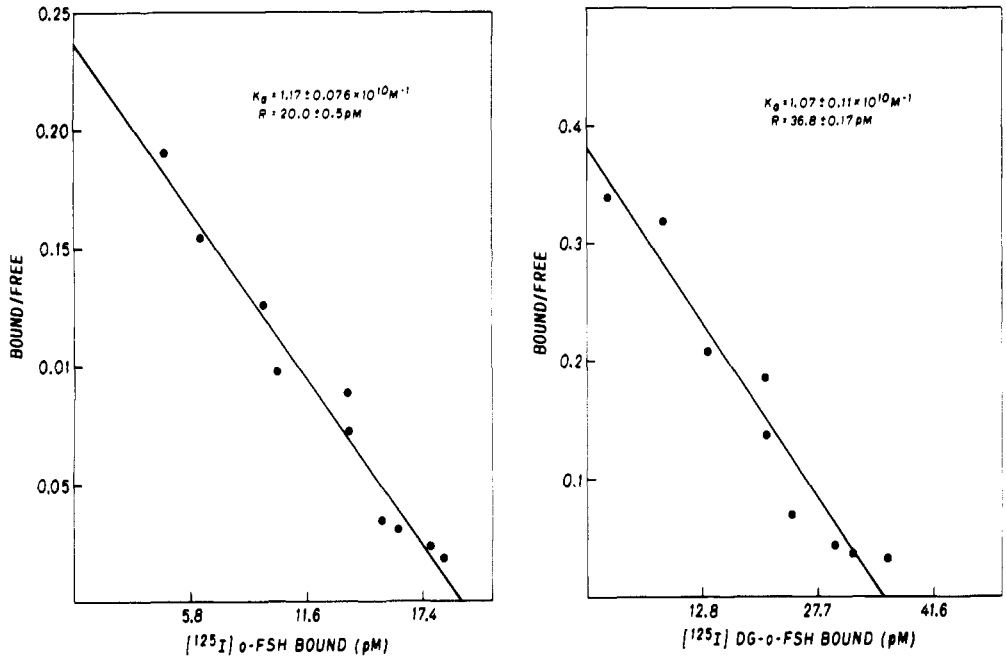

FIGURE 3: Scatchard plot derived by incubating the porcine ovarian P1 fraction membrane with increasing concentrations of ^{125}I-oFSH or ^{125}I-DG-oFSH. Binding was assayed over the range 28.0 pM (0.25 ng) to 985 pM (8.4 ng) total added ^{125}I-oFSH (85 μCi/μg) or 10.4 pM (0.075 ng) to 1138 pM (8.2 ng) ^{125}I-DG-oFSH. The incubation period was 6 h at 37 °C for oFSH and 1.3 h for DG-oFSH. Each assay tube contained tracer, assay buffer (pH 7.2) consisting of 25 mM Tris-HCl, 10 mM $MgCl_2$, and 0.1% BSA, and ≈30 μg of P1 fraction protein ± 500 ng of unlabeled hormone. Computer analysis estimated (for oFSH) a K_A and K_D at (1.17 ± 0.076) × 10^{10} M^{-1} and 85.4 pM, respectively, with a binding capacity (R) of 27.7 ± 4.37 pM (n = 4). The respective values for DG-oFSH (n = 3) are (1.07 ± 0.11) × 10 M^{-1}, 93.4 pM, and 36.8 ± 0.17 pM.

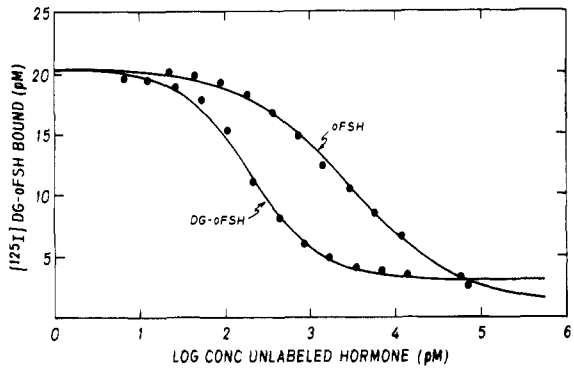

FIGURE 4: Inhibition of binding of ^{125}I-DG-oFSH by unlabeled DG-oFSH and oFSH to porcine granulosa cell membranes. The experiments were performed with 74.2 pM ^{125}I-DG-oFSH (68 574 cpm), ≈41 μg protein equivalent of P1 fraction, and varying concentrations of unlabeled oFSH or DG-oFSH in a total volume of 300 μL of assay buffer. Nonspecific binding was determined in the presence of 58.4 or 69.4 nM unlabeled oFSH or DG-oFSH, respectively. The incubation period was 2.5 h at 37 °C. Each value represents the mean of triplicate determinations. The curve was computed as the best fit to the experimental data by nonlinear least-squares curve-fitting methods. The DG-oFSH curve has a slope of 0.979 ± 0.101. The IC_{50} is estimated at 195 ± 33 pM. The slope factor and IC_{50} of the oFSH computer-fitted curve are 0.673 ± 0.058 and 2850 ± 290 pM. Of the ^{125}I-DG-oFSH added, 27.8% is totally bound (20.7 ± 0.94 pM). The DG-oFSH competition curve has a $K_A \approx (1.2 \pm 0.2) \times 10^{10}$ M^{-1} and an R value of 47 ± 4 pM.

bation period (data not shown) where "theoretically" attainment of equilibrium binding for unlabeled oFSH is to occur on the basis of analysis of association kinetics of ^{125}I-labeled oFSH, since an asymptotic plateau in the binding of the tracer at this time (data not shown) is observed. On the basis of a number of experiments under equilibrium binding conditions, at 37 °C, a slope factor near unity was observed (i.e., 0.977 ± 0.02, n = 4). Analysis indicated an equilibrium binding constant for only a high-affinity binding site equal to (0.72 ± 0.19) × 10^{10} M^{-1} (n = 4), with a binding capacity of 63 ± 11 pM. Interestingly, unlabeled oFSH bound only 56% of the total binding sites available to unlabeled DG-oFSH (112 ± 22 pM; n = 3) on the basis of ^{125}I-oFSH/DG-oFSH competition curves under identical assay conditions. In contrast to oFSH curves, DG-oFSH displacement curves generally had hypersteep slope factors (i.e., 1.46 ± 0.15, n = 4). Figure 6 shows a typical experiment where unlabeled DG-oFSH competes for binding with ^{125}I-oFSH. Under such conditions, the fast equilibrating competitor is at equilibrium relative to the binding of the slow competing ^{125}I-oFSH. If the latter is allowed to attain equilibrium, no marked changes occur in the slope factor of ^{125}I-oFSH/DG-oFSH curves (data not shown). Under these assay conditions, an estimated K_A for unlabeled DG-oFSH was approximately 6.39 ± 0.75 (n = 3).

Analysis of ^{125}I-Labeled oFSH and DG-oFSH Dissociation Binding Data. To determine the nature of dissociation, granulosa cell membrane P1 fraction was incubated with ^{125}I-labeled oFSH or DG-oFSH for 80 min at 37 °C to promote the formation of the hormone receptor complex. Following this period, a large excess of unlabeled homologous hormone (agonist–agonist/antagonist–antagonist) was added to the reaction vessel to induce dissociation of prebound radiolabeled tracer. A representative dissociation experiment for oFSH and DG-oFSH is indicated in Figure 7. In the presence of excess blocker, both radiolabeled ligands demonstrate reversible interactions with the receptor. Under these conditions, dissociation of both tracers follows a biexponential rate of dissociation. Analysis of data from two experiments, using different tracers and membrane preparations, reveals ≈20% of prebound ^{125}I-oFSH dissociates rapidly with a half-time equal to ≈22 min. A second slower decrement in dissociation occurs with a half-time in terms of hours (≈18 h, range 11–24 h) comprising the remainder of total prebound ^{125}I-oFSH.

The pool of prebound ^{125}I-DG-oFSH that rapidly dissociates in the presence of excess unlabeled ligand consists of ≈23%. This dissociation is best described by a half-time in terms of

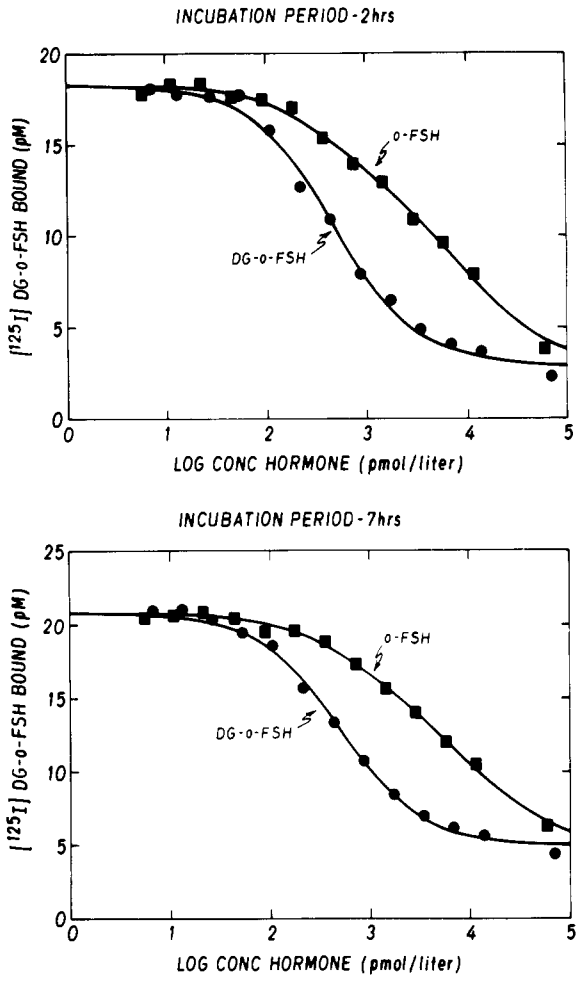

FIGURE 5: Lack of effect of duration of incubation at 37 °C on the ^{125}I-DG-oFSH competition binding assay performed in the presence of titrated amounts of oFSH and DG-oFSH. The receptor binding assay was performed as indicated in the text. Specifically, the incubate (300 μL) contained ≈56 221 cpm (65 pM/0.47 ng) of ^{125}I-DG-oFSH ± various amounts of unlabeled homologous competitor, assay buffer, and porcine granulosa cell membranes (≈60 μg of protein equivalent). Nonspecific binding was determined in the presence of 500 ng of unlabeled competitor. After a 2-h incubation, DG-oFSH has a slope of 1.0 ± 0.09 and an R value of 97.2 ± 9.2 pM. The 7-h incubate gave a slope of 0.99 ± 0.60 and an R value of 113 ± 11 pM. oFSH competition assay at 2 h resulted in a slope and high (R_H) and low (R_L) binding capacities of 0.63 ± 0.07, 46 ± 13 pM, and 55 ± 12 pM, respectively, vs. 7-h values of 0.68 ± 0.06, 54 ± 15 pM, and 64 ± 14 pM, respectively.

minutes, ≈32 min (range 23–41 min). The remaining dissociable pool of ^{125}I-DG-oFSH has a half-time in hours (≈44 h, range 20–67 h). As is the case with oFSH, where the fast and slow dissociation rate constants are estimated at 3.2×10^{-2} min^{-1} [range $(3.1–3.2) \times 10^{-2}$ min^{-1}] and 0.78×10^{-3} min^{-1} [range $(0.47–1.1) \times 10^{-3}$ min^{-1}], DG-oFSH also dissociated biexponentially. The fast and slow K_{off} estimates are 2.3×10^{-2} min^{-1} [range $(1.7–3.0) \times 10^{-2}$ min^{-1}] and 3.7×10^{-4} min^{-1} [range $(1.7–5.7) \times 10^{-4}$ min^{-1}], respectively. Although the fast rates of release of the bound ^{125}I-ligands from their respective binding sites are similar, DG-oFSH shows a longer half-time for the slower dissociation vs. oFSH. DG-oFSH's slower dissociation half-time is approximately 2 times longer than that of oFSH.

Determination of the Reversibility of oFSH and DG-oFSH Binding as a Function of Reaction Time. It is assumed that following the 30- or 120-min preincubation period, addition of excess (1000 ng) homologous hormone at these time points eliminates the forward reaction and what is essentially being

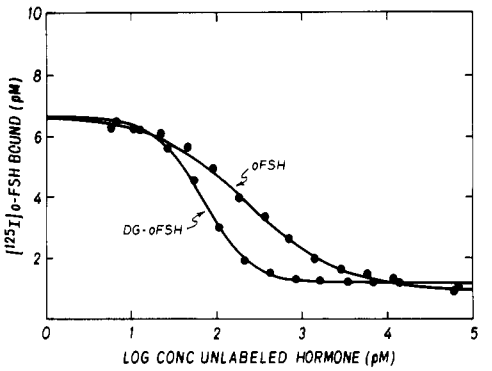

FIGURE 6: Binding inhibition curves of unlabeled DG-oFSH and oFSH for the binding of ^{125}I-oFSH to porcine ovarian P1 fraction under nonequilibrium conditions. The incubate (300 μL) contained ≈41 μg of protein equivalent of P1 fraction, 44.2 pM ^{125}I-oFSH (66 395 cmp), various doses of unlabeled oFSH (5.6 pM–58.4 nM) or DG-oFSH (6.6 pM–69.4 nM), and assay buffer. Nonspecific binding was determined in the presence of a 500-fold excess of oFSH (58.4 nM) or DG-oFSH (69.4 nM). In the absence of any unlabeled hormone, 15.0% ^{125}I-oFSH added is specifically bound (6.7 pM). Data represent the mean of triplicate values. The IC_{50} values for the DG-oFSH and oFSH curves are 69.8 ± 5.3 and 241 ± 45 pM, respectively. The incubation period was 2.5 h at 37 °C.

analyzed is the reverse reaction process. During the entire dissociation period, analysis of the association kinetics revealed no loss of specific binding (figure not shown). As previously observed, dissociation of both labeled ligands from the P1 fraction is extremely slow and is not a readily reversible biexponential process. On the basis of two experiments each using two separately prepared membrane preparations and labeled hormones, an average of 39% (range 37–40%) and 45% (range 40–48%) of the easier dissociable pool of prebound ^{125}I-DG-oFSH and ^{125}I-oFSH is displaced. For estimates of the time constant of dissociation (min^{-1}) at 30-min-induced dissociation, the fast components of dissociation of both hormone and analogue are similar, i.e., 1.2×10^{-2} min^{-1} [range $(1.0–1.3) \times 10^{-2}$ min^{-1}] and 1.5×10^{-2} min^{-1} [range $(1.1–1.8) \times 10^{-2}$ min^{-1}] for DG-oFSH and FSH, respectively. If the association period is extended up to the 2-h period, the amount of dissociation of prebound ^{125}I-DG-oFSH and ^{125}I-oFSH is reduced to 25% (range 24–26%) and 29% (range 26–32%), respectively. There is a definite difference in the amount of ligand dissociating from receptor that is related to the time allowed for the reaction to occur. Allowing the association reaction to proceed for an additional 90 min did not alter the fast time constant for dissociation. The slower dissociation process time constant could not be estimated at either 30- or 120-min-induced dissociation time since curve-fitting methods revealed an infinitely slow dissociation process for the slower component.

Discussion

The pituitary and placental glycoprotein hormones are unique among hormones not only because of their complex oligosaccharide structures but also because of their facile conversion into competitive antagonists by a one-step removal of accessible carbohydrate moieties (Manjunath & Sairam, 1984; Sairam et al., 1983). As such modified analogues are not available for any other large protein hormone, the present study represents an example of large agonist/antagonist–receptor interactions.

The first step in the analysis of a ligand–receptor system is to perform a "kinetic" or time study on the rates of association and dissociation of radiolabeled ligands. These data should then be used to design equilibrium binding experiments.

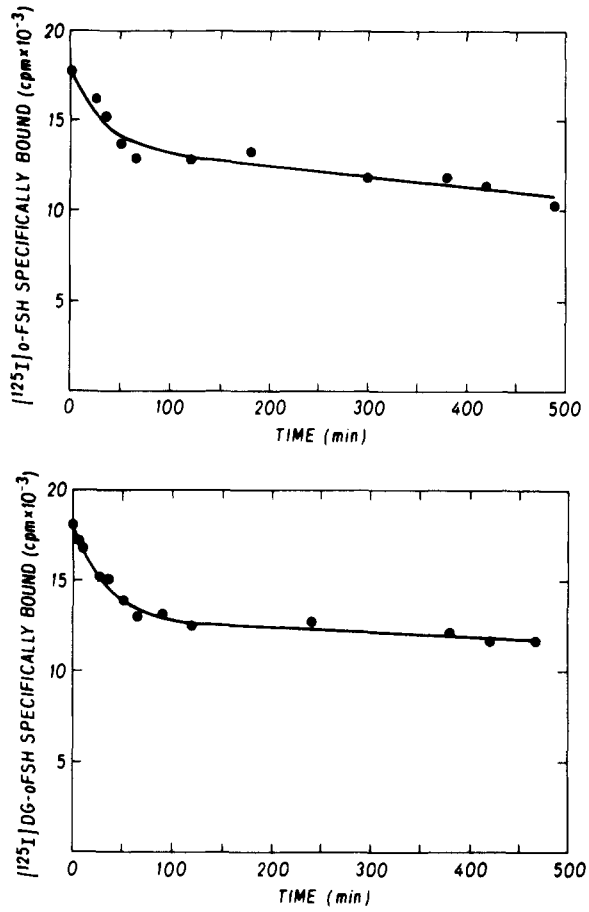

FIGURE 7: Time course of dissociation, at 37 °C, of ^{125}I-oFSH (top panel) and ^{125}I-DG-oFSH (bottom panel) to porcine ovarian P1 fraction receptors. Dissociation of both ^{125}I-labeled ligands was determined after allowing 80 min for biding to occur. Sufficient tracer, receptor, and assay buffer were added to reaction vessels such that 300 μL could be removed from the reaction medium as a function of time to determine separately nonspecific, total binding and the degree of dissociation. The incubates contained, per milliliter of reaction mixture volume, 4 ng of ^{125}I-oFSH or 1.4 ng of ^{125}I-DG-oFSH, 136 μg of P1 fraction protein, and assay medium as described under Materials and Methods. At zero-minute dissociation, 5.2 μg of unlabeled DG-oFSH or oFSH was added to a final concentration of 138 nM (1000 ng) and 117 nM (1000 ng) per 300 μL. Of the total tracer added, 11.9% ^{125}I-oFSH (17 784 cpm) and 23.0% ^{125}I-DG-oFSH (18 120 cpm) were specifically bound at t = 0-min dissociation. This represents 79% and 82% specific binding, respectively. There was no loss of binding for both ligands as determined from the association isotherm. Data points are the mean of triplicate determinations.

The kinetics of gonadotropin–receptor binding have not been more extensively studied and quantified than steady-state (equilibrium) binding analysis of such ligands. To our knowledge, the findings reported here and earlier preliminary work (Sebok et al., 1985) constitute the first characterization of oFSH and deglycosylated oFSH binding to porcine granulosa cell membranes. Computer analysis of the association binding curves of ^{125}I-oFSH at 37 °C is best described by a biexponential rate equation. There are two exponential components of binding; the amount of bound iodotracer in each is approximately equal. Measurement of ^{125}I-DG-oFSH kinetics reveals a disproportionate amount of the two components; a major amount of the total bound tracer is associated with the component described by a fast rate of association, and the remainder, <27% at most when present (Figure 1), is represented by a slower association rate. For both labeled hormones, these two rates of association are independent of ligand concentration (Figure 2), suggesting that binding is not a diffusion-controlled process and does not follow a simple bimolecular reaction scheme as would be proposed by the single occupancy model (Burgen et al., 1975). If we assume that the velocity of binding of both ligands is controlled by orientation or conformational restrictions, it is possible that DG-oFSH binds with a faster rate of association due to a lack of steric hindrance and therefore is at the correct conformation (and therefore correct orientation) facilitating binding, assuming, of course, a single-step binding event. We are of the opinion that since both labeled hormones demonstrate complex association kinetics, more so with oFSH than DG-oFSH, the association of ligand to binding sites is a complex reaction. If one assumes a "sequential model" of hormone–receptor interaction (De Lêan et al., 1979), it is possible that conformational rearrangement of the "free" portion of bound DG-oFSH occurs more readily because of less steric hindrance, allowing the sequential binding steps to occur faster.

In order to gain more insight into the "nature and differences" of interaction of these ligands with the FSH receptor contained in the P1 fraction of the membranes, we compared competition and saturation curves. We have used the novel deglycosylated analogue of oFSH along with the application of computer-modeling techniques shown to work for small ligands such as the β-receptor system (De Lêan et al., 1979) to characterize the FSH receptor binding properties. Scatchard analysis and homologues competition assays performed at 37 °C revealed that the iodinated form of both ovine follitropin and unlabeled oFSH is recognized by the receptor with equal affinity. This observation was also true with deglycosylated oFSH. Scatchard transformation of the binding data from saturation experiments resulted in a straight line for both radiolabeled tracers, indicative of high-affinity binding to a set of thermodynamically equivalent sites. We conclude that the equilibrium association constant of the high-affinity binding sites for both ligands, estimated at $\approx 1.0 \times 10^{10}$ M^{-1}, and the binding capacities are equivalent. Homologous displacement binding assays revealed that oFSH and DG-oFSH curves, at equilibrium binding conditions, result in curves having "normal" steepness consistent with the notion of a population of FSH receptors having equal affinity for the ligand. The equilibrium binding constant [$K_A \approx (0.72 \pm 0.19) \times 10^{10}$ M^{-1}] estimated for oFSH was similar to that from Scatchard analysis [$K_A \approx (0.94 \pm 0.21) \times 10^{10}$ M^{-1}]. DG-oFSH saturation and competitive binding assays gave estimates of the K_A that were not markedly different, $K_A = (1.22 \pm 0.11)$ and $(0.86 \pm 0.18) \times 10^{10}$ M^{-1}, respectively. Although a homogeneous class of high-affinity binding sites were characterized for oFSH based on homologous saturation and competition assays, such an observation is inconsistent with heterologous displacement assays. oFSH displaces DG-oFSH from its binding site in a complex manner. This is not due to a lack of equilibrium. Although it has been documented that competition patterns change with time (Arányi, 1980), this phenomenon was not markedly noticed in ^{125}I-DG-oFSH competition assays. Our results do not provide an explanation for "shallow" agonist competition curves. Several proposed models (De Lêan, 1984; De Lêan et al., 1979, 1982) of ligand–receptor interaction may be applicable to our findings. In a two-site receptor model (De Lêan et al., 1982), it is implicitly indicated in the analysis that antagonist binding to two classes of sites is of equal affinity. Using this priori, we can best describe the concentration-dependent inhibition of ^{125}I-DG-oFSH binding by oFSH with a two-site model vs. a one-site receptor model. The diminution in the residual sum of squares from a one-site vs. a two-site model is highly significant. Evidently, oFSH binds to a site of high affinity (K_A

$\approx 10^{10}$ M^{-1}) and a site of low affinity ($K_A \approx 10^8$ M^{-1}), the proportions being near equal. Furthermore, the sum of the independent binding capacities equals that of ^{125}I-DG-oFSH. This observation is unique in that the association kinetics of oFSH reveal two components in the association binding curves that also are of near equal proportion (i.e., 50%/50%).

Measurement of the kinetics of dissociation prior to reaching equilibrium binding revealed multiple-order K_{off} values for the reaction scheme for both radiolabeled tracers regardless of the two experimental approaches used. This observation is suggestive of the presence of multiple receptors or a slow reversible binding reaction that is complex. Displacement of the bound ^{125}I-labeled oFSH and DG-oFSH by excess homologous hormone is not completely dissociable under these experimental conditions. The removal of prebound tracer requires many hours, as unlabeled homologous hormone can competitively displace the labeled hormone by approximately two-thirds in 6 h. At least two components consisting of a fast and a slow rate of dissociation are involved for both ^{125}I-labeled oFSH and DG-oFSH.

The findings on dissociation kinetics for FSH concur with the observations made with bull (Cheng, 1975), calf (Abou-Issa & Reichert, 1977), porcine (Maghuin-Rogister et al., 1978), monkey (Berman & Sairam, 1982), and rat (Abou-Issa & Reichert, 1976) testicular tissue and with rat granulosa cells (Nimrod et al., 1976). Such slow complex dissociation kinetics are also characteristic of other glycoprotein ligands such as lutropin (Lee & Ryan, 1973; Liu et al., 1984). Analysis of DG-oFSH dissociation curves into components reveals its major, but slower, exponential components decay with a $t_{1/2}$ approximately 2 times longer than oFSH. Both ligands have $t_{1/2}$ values for the rapidly but minor dissociating component that are similar. Both ligands demonstrate changes in the ratio between the size of the fast and slow components in relation to the binding reaction time; however, these changes are similar for both ligands. On the basis of these findings and association kinetic data, it is hypothesized that there is a complex multistep binding process and/or isomerization sequence with two or more steps that may be due to conformational changes. Our analysis does not allow us to discriminate if receptor and/or ligand is involved in these events. Since the events are time related, they result in the conversion of a "loosely" bound form of the ligand–receptor complex to a thermodynamically more stable form (i.e., tighter) of the complex; therefore, bound ligand becomes less displaceable by cold hormone as a function of time. Ths concurs with similar observations for the testicular FSH (Maghuin-Rogister et al., 1978) and LH (Katikineni et al., 1980) and for ovarian LH (Lee & Ryan, 1973) receptor systems. Since radiolabeled FSH demonstrates a complex binding reaction, more so than DG-oFSH, both of which are not simple bimolecular events, it is difficult to derive absolute "rate" constants based on data from nonequilibrium and equilibrium experiments.

It should be noted that the use of principles based on the law of mass action is not as easily applicable to large and complex ligands, such as FSH and LH. Therefore, our interpretation of the data presented here can be considered as first approximations to help compare the underlying different molecular binding events of these ligands using porcine granulosa cell membrane fractions. Experimental data presented here support the notion of two distinct, noninteracting binding sites that vary in affinity and binding capacity. Whether these are separate sites or sites on the same receptor has yet to be determined. We conclude that DG-oFSH binds to these sites with equal affinity whereas oFSH binds to these sites with unequal affinity. Interestingly, Reichert and colleagues (Dias et al., 1981; Reichert et al., 1982) have proposed a model whereby each FSH receptor contains two noninteracting binding sites for the binding of two molecules of FSH. On the basis of observations of De Lêan et al. (1979), it is possible that the heterogeneity of binding observed for oFSH in heterologous competition assays may not be interpreted as such, but rather as a single class of binding sites. We rule out this interpretation on the basis of our kinetic data. One can speculate that the underlying lack of full agonist potency (Sairam, 1985) of deglycosylated gonadotropins, as exemplitified by DG-oFSH in this study, may be explained in part by their differential binding characteristics.

ACKNOWLEDGMENTS

The supply of pig follicular fluid by the Contraceptive Development Branch of NICHHD is gratefully acknowledged.

Registry No. FSH, 9002-68-0.

REFERENCES

Abou-Issa, H., & Reichert, L. E., Jr. (1976) *J. Biol. Chem. 251*, 3326–3337.

Abou-Issa, H., & Reichert, L. E., Jr. (1977) *J. Biol. Chem. 252*, 4166–4174.

Anderson, T. T., & Reichert, L. E., Jr. (1982) *J. Biol. Chem. 257*, 11551–11557.

Arânyi, P. (1980) *Biochim. Biophys. Acta 628*, 220–227.

Berman, M. I., & Sairam, M. R. (1982) *J. Clin. Endocrinol. Metab. 55*, 1153–1160.

Berman, M. I., & Sairam, M. R. (1983) *Can. J. Biochem. Cell. Biol. 61*, 561–568.

Berman, M. I., & Sairam, M. R. (1984) *J. Reprod. Fertil. 70*, 463–471.

Berman, M. I., Anand-Srivastava, M., & Sairam, M. R. (1985) *Mol. Cell. Endocrinol. 42*, 49–57.

Bhalla, V. K., & Reichert, L. E., Jr. (1974) *J. Biol. Chem. 249*, 43–51.

Burgen, A. S. V., Roberts, G. C. K., & Feency, J. (1975) *Nature (London) 253*, 753–755.

Cheng, K. (1975) *Biochem. J. 149*, 123–132.

Davies, A. G., Lawrence, N. R., & Lynch, S. S. (1978) *J. Reprod. Fertil. 53*, 249–254.

De Lêan, (1984) in *Computers in Endocrinology* (Rodbard, D., & Forti, G., Eds.) pp 147–161, Raven Press, New York.

De Lêan, A., Munson, P. J., & Rodbard, D. (1978) *Am. J. Physiol. 235*, E97–E102.

De Lêan, A., Munson, P., & Rodbard, D. (1979) *Mol. Pharmacol. 15*, 60–70.

De Lêan, A., Hancock, A. A., & Lefkowitz, R. J. (1982) *Mol. Pharmacol. 21*, 5–16.

Dias, J. A., Treble, D. H., Bennett, A. H., & Reichert, L. E. (1981) *J. Androl. 5*, 259–268.

Dias, J. A., Huston, J. S., & Reichert, L. E., Jr. (1984) *Endocrinology (Baltimore) 114*, 1259–1265.

Feldman, H. A. (1972) *Anal. Biochem. 48*, 317–338.

Fletcher, P. W., & Reichert, L. E., Jr. (1984) *Mol. Cell. Endocrinol. 34*, 39–49.

Katikineni, M., Davies, T. T., Huhtaniemi, I. T., & Catt, K. J. (1980) *Endocrinology (Baltimore) 107*, 1980–1987.

Labarbera, A. R., & Ryan, R. J. (1981) *Endocrinology (Baltimore) 108*, 1561–1570.

Lee, C. Y., & Ryan, R. J. (1973) *Biochemistry 12*, 4609–4615.

Liu, W. K., Young, J. D., & Ward, D. N. (1984) *Mol. Cell. Endocrinol. 37*, 29–30.

Louvet, J., & Vaitukaitis, J. (1976) *Endocrinology (Philadelphia) 99*, 758–764.

Maghuin-Rogister, G., Closset, J., Combarnous, Y., Hennen, G., Dechenne, C., & Ketelslegers, J. (1978) *Eur. J. Biochem. 86*, 121-131.
Manjunath, P., & Sairam, M. R. (1984) *Methods Enzymol. 109*, 725-735.
Manjunath, P., Sairam, M. R., & Sairam, J. (1982) *Mol. Cell. Endocrinol. 28*, 125-138.
Means, A. R., & Vaitukaitis, J. (1972) *Endocrinology (Philadelphia) 90*, 39-46.
Midgley, A. R. (1973) *Adv. Exp. Med. Biol. 36*, 365-378.
Munson, P. J., & Rodbard, D. (1980) *Anal. Biochem. 107*, 220-239.
Nakano, R., Akahori, T., Katayama, K., & Tojo, S. (1977) *J. Reprod. Fertil. 51*, 23-27.
Nimrod, A., Erickson, G., & Ryan, K. J. (1976) *Endocrinology (Philadelphia) 98*, 56-64.
O'Neill, C. W., & Reichert, L. E., Jr. (1984) *Endocrinology (Baltimore) 114*, 1135-1140.
Reichert, L. E., & Bhalla, V. K. (1974) *Endocrinology (Philadelphia) 94*, 483-491.
Reichert, L. E., & Ramsey, R. B. (1975) *J. Biol. Chem. 250*, 3034-3040.
Reichert, L. E., Dias, J. A., Fletcher, P. W., & O'Neill, W. L. (1982) *Ann. N.Y. Acad. Sci. 383*, 135-150.
Sairam, M. R. (1979a) *Arch. Biochem. Biophys. 194*, 63-70.
Sairam, M. R. (1979b) *J. Endocrinol. 82*, 253-262.
Sairam, M. R. (1985) in *The Receptors* (Conn, P. M., Ed.) Vol. 11, pp 307-340, Academic Press, New York.
Sairam, M. R., & Manjunath, P. (1982a) *Mol. Cell. Endocrinol. 28*, 139-150.
Sairam, M. R., & Manjunath, P. (1982b) *Mol. Cell. Endocrinol. 28*, 151-159.
Sairam, M. R., Manjunath, P., Sairam, J., & Dobias-Goff, M. (1983) in *Factors Regulating Ovarian Function* (Greenwood, G. S., & Terranova, P. F., Eds.) pp 317-321, Raven Press, New York.
Salhanick, A. I. (1980) *Life Sci. 26*, 2281-2288.
Sebok, K., De Lēan, A., & Sairam, M. R. (1985) *Endocrinology (Baltimore) 116 (Suppl.)*, 1134.
Stewart, F., & Allen, W. R. (1979) *J. Reprod. Fertil. 27*, 431-440.
Thanki, K. H., & Steinberger, A. (1978) *Andrologia 10*, 195-202.

Identification of Cytochrome *b* and a Molecular Weight 12K Protein as the Ubiquinone-Binding Proteins in the Cytochrome b–c_1 Complex of a Photosynthetic Bacterium *Rhodobacter sphaeroides* R-26†

Linda Yu and Chang-An Yu*

Department of Biochemistry, Oklahoma State University, Stillwater, Oklahoma 74078

Received October 1, 1986; Revised Manuscript Received January 16, 1987

ABSTRACT: An azidoubiquinone derivative, 3-azido-2-methyl-5-methoxy-6-(3,7-dimethyloctyl)-1,4-benzoquinone, was used to study the ubiquinone–protein interaction and to identify ubiquinone-binding proteins in photosynthetic bacterial cytochrome b–c_1 complex. When isolated *Rhodobacter sphaeroides* cytochrome b–c_1 complex is incubated with a 50-fold molar excess of the azidoubiquinone derivative in the dark, no loss of activity is observed. Photolysis of this azidoubiquinone-treated sample for 5 min at 0 °C causes a 50% decrease of ubiquinol–cytochrome *c* reductase activity. When the photolyzed [^{3}H]azidoubiquinone-treated *R. sphaeroides* cytochrome b–c_1 complex is subjected to sodium dodecyl sulfate–polyacrylamide gel electrophoresis, after removal of non-protein-linked azidoubiquinone by organic solvent extraction, followed by analysis of the radioactivity distribution among subunits of the complex, cytochrome *b* (M_r 43K) and a M_r 12K protein are heavily labeled, suggesting that these two proteins are the ubiquinone-binding site in this complex. The amount of radioactivity in both proteins is increased when the complex is subjected to phospholipase A_2 digestion prior to photolysis with the azidoubiquinone derivative. Pretreatment of *R. sphaeroides* cytochrome b–c_1 complex with 2-heptyl-4-hydroxyquinoline *N*-oxide has little effect on the distribution of radioactivity among subunits of the cytochrome b–c_1 complex. Pretreatment of the cytochrome b–c_1 complex with 5-*n*-undecyl-6-hydroxy-4,7-dioxobenzothiazole, myxothiazol, or antimycin increases slightly the amount of radioactivity in cytochrome *b*. These results suggest that the active site of these inhibitors is not the same as the Q-binding site.

The cytochrome b–c_1 complex (formerly known as the cytochrome b–c_2 complex) of the photosynthetic bacterium *Rhodobactor sphaeroides*, which catalyzes electron transfer from ubiquinol to cytochrome c_2, has recently been purified and characterized in several laboratories (Gabellini et al., 1982; Yu & Yu, 1982; Yu et al., 1984; Takamiya et al., 1982; Ljungdahl et al., 1986). The essential redox components of this complex are identical with those of the mitochondrial cytochrome b–c_1 complex (Cramer & Crofts, 1982; Hauska et al., 1983). They are cytochromes *b* and c_1, iron–sulfur protein, and ubiquinone. Purified *R. sphaeroides* cytochrome

† This work was supported in part by the USDA (Grant GAM 8400640) and Oklahoma Agricultural Experimental Station (J-5079).

0006-2960/87/0426-3658$01.50/0